Optimal Supply Chain Design and Operations Under Multi-Scale Uncertainties: Nested Stochastic Robust Optimization Modeling Framework and Solution Algorithm

Dajun Yue and Fengqi You
Dept. of Chemical and Biological Engineering, Northwestern University, Evanston, IL 60208

DOI 10.1002/aic.15255
Published online April 14, 2016 in Wiley Online Library (wileyonlinelibrary.com)

Although strategic and operational uncertainties differ in their significance of impact, a "one-size-fits-all" approach has been typically used to tackle all types of uncertainty in the optimal design and operations of supply chains. In this work, we propose a stochastic robust optimization model that handles multi-scale uncertainties in a holistic framework, aiming to optimize the expected economic performance while ensuring the robustness of operations. Stochastic programming and robust optimization approaches are integrated in a nested manner to reflect the decision maker's different levels of conservativeness toward strategic and operational uncertainties. The resulting multi-level mixed-integer linear programming model is solved by a decomposition-based column-and-constraint generation algorithm. To illustrate the application, a county-level case study on optimal design and operations of a spatially-explicit biofuel supply chain in Illinois is presented, which demonstrates the advantages and flexibility of the proposed modeling framework and efficiency of the solution algorithm. © 2016 American Institute of Chemical Engineers *AIChE J*, 62: 3041–3055, 2016
Keywords: multi-scale uncertainties, stochastic robust optimization model, column-and-constraint generation algorithm, supply chain optimization

Introduction

When hedging against uncertainties in the optimal design and operations of supply chains, only one uniform approach has been typically used to tackle all types of uncertainty.[1–3] This "one-size-fits-all" approach might be stochastic programming, robust optimization, fuzzy programming, or any other methods for optimization under uncertainty.[4] However, uncertainties at strategic and operational scales may differ in their significance of impact,[5] as shown in Figure 1. Strategic uncertainties have impacts over a significant duration of the project's lifetime. Once realized, strategic uncertainties would remain unchanged for a considerable period of time. Examples of strategic uncertainties include climate and weather, technology evolution, incentives and policies, and network stability. In contrast, operational uncertainties change more frequently and often lead to immediate adjustment in operational decisions. Examples of operational uncertainties include variations in raw material quality and composition, supply and demand, cost and price, as well as in lead times of production, transportation, and material handling activities. Moreover, the realizations of operational uncertainties may be associated with that of strategic uncertainties. For example, the yields of agricultural products are expected to be dependent on the climate and weather. In addition, a decision maker may hold different levels of conservativeness toward strategic and operational uncertainties. For instance, one might be less conservative toward strategic uncertainties and willing to explore the potentials of all possibilities, but be more conservative toward operational uncertainties considering factors such as demand fulfill rate.

Due to all the concerns above, a "one-size-fits-all" approach may not be sufficient for efficiently handling multi-scale uncertainties in optimal design and operations of supply chains. Therefore, a heterogeneous modeling framework is required. Consequently, the goal of this work is to propose a holistic modeling framework and solution algorithm to handle both strategic and operational uncertainties for supply chain optimization problems. We aim to obtain "here-and-now" decisions for supply chain design that has the optimal expected economic performance (e.g., minimum cost, maximum net present value), and simultaneously ensures the robustness of future operations given the recourse in a "wait-and-see" manner. Different methods for optimization under uncertainty have their respective scopes of application.[4] Considering the case that a decision maker is less conservative toward strategic uncertainties and more conservative toward operational uncertainties, we select stochastic programming and robust optimization approaches for modeling strategic and operational uncertainties, respectively. To integrate stochastic programming and robust optimization approaches in a holistic framework, we propose a stochastic robust optimization model that couples the two approaches in a nested manner. The different levels of conservativeness of the decision maker and interactions between the strategic and

Correspondence concerning this article should be addressed to F. You at you@northwestern.edu.

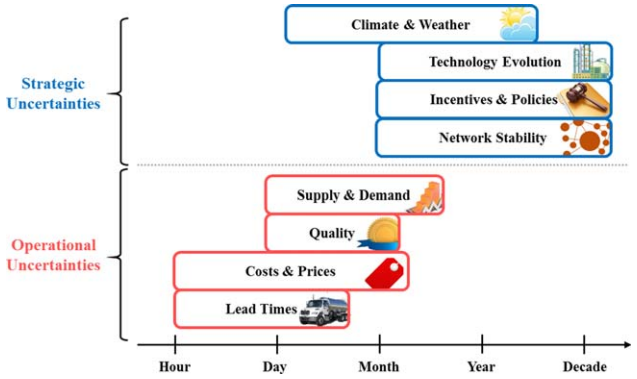

Figure 1. Illustration of multi-scale uncertainties in supply chain design and operations.

[Color figure can be viewed in the online issue, which is available at wileyonlinelibrary.com.]

operational uncertainties are explicitly accounted for. The resulting model is formulated as a multi-level (e.g., min–max–min) mixed integer linear program (MILP), involving both the expectation over multiple scenarios[6] as well as the max–min function.[7] Since this multi-level MILP cannot be solved directly by any off-the-shelf solver, we further propose an improved decomposition-based column-and-constraint generation (C&CG) algorithm[8] for its solution. The improved C&CG algorithm is based on a single-master-problem-multi-subproblems framework, instead of the original single-master-problem-single-subproblem framework. To illustrate the applicability of the proposed modeling framework and solution algorithm, we present a county-level case study on optimal design and operations of a spatially-explicit biofuel supply chain in Illinois. Comparison with conventional approaches, including the deterministic model and standard two-stage stochastic programming approach, is performed to demonstrate the advantages and flexibility of the proposed approach.

Major novelties of this work are summarized below:

- A novel framework that distinguishes and handles uncertainties at multiple scales in optimal design and operations of supply chains;
- Modeling of the different characteristics of and the decision maker's different levels of conservativeness toward strategic and operational uncertainties;
- A nested stochastic robust optimization framework that integrates stochastic programming and robust optimization approaches in contrast to a uniform approach;
- An improved decomposition-based C&CG algorithm that efficiently solves the resulting multi-level MILP problem.

The rest of this article is organized as follows. We briefly review relevant literature in the next section. We then present the general problem statement and model formulation, followed by the solution strategy employed to tackle the problem. The case study on biofuel supply chain is provided at the end to demonstrate the application.

Literature Review

There are many comprehensive reviews covering the topic of supply chain design and operations under uncertainty.[3,9–11] In this section, we mainly review the literature that employ mathematical programming approaches to explicitly account for supply chain uncertainties.

The most widely used approach is two-stage stochastic programming,[6,12] where the first-stage and second-stage variables correspond to supply chain design and operational decisions, respectively. Various types of uncertainty, including supply, demand, freight rate, cost, price, and outcome of clinical trials, have been successfully handled by stochastic programming approach,[13–17] aiming to optimize the expected economic performance of supply chains. To tackle the challenge of exponential growth in the number of scenarios, Monte Carlo sampling and Sample Average Approximation method have been commonly adopted.[18–22] While stochastic programming reflects a risk-neutral attitude of the decision maker, chance-constrained programming approach can be employed to improve the reliability of supply chains by imposing a minimum requirement on the probability of satisfying constraints.[23,24] The chance-constrained approach has been used to handle the trade-off between customer demand satisfaction and production cost[25,26] and uncertainties in damage model parameters for sustainability analysis.[27] In cases that the decision maker values feasibility higher than optimality, adaptive robust optimization can be used to hedge against the worst case of uncertainty realization.[28,29] The robust optimization approach reflects the decision maker's conservativeness in supply chain design and operations. Applications of robust optimization approach include network design,[30,31] contracting[32] and pricing problems.[33] Another approach to model supply chain uncertainties is fuzzy programming,[34,35] where random parameters are considered as fuzzy numbers and constraints are treated as fuzzy sets. Conversion rate, cost, supply and demand have been modeled as fuzzy numbers to account for data uncertainty in supply chain design and operations.[36–38] There are also dedicated supply chain models developed for specific types of uncertainties. Reliable facility location models have been proposed to consider unexpected failure of plants or warehouses, as well as possible customer reassignment.[39,40] Stochastic inventory models have been introduced to handle supply delays and demand variations through simultaneous optimization of production plans and inventory placement.[41–46] Incorporating uncertainty metrics (e.g., downside risk[47] or conditional value at risk[48,49]) in addition to the traditional economic criteria in a multi-objective optimization framework has been undertaken to address risk management in supply chain optimization.[21,50–52]

A few researchers have combined different methods for optimization under uncertainty to leverage the respective advantages and complement the corresponding drawbacks. A weighted sum of stochastic programming and robust optimization objectives has been considered as the objective to reflect the decision maker's preference between feasibility and optimality.[53] Stochastic robust formulations have been proposed for strategic supply chain optimization under uncertainty.[54,55] In such formulations, each scenario is associated with a set of uncertainty realizations instead of a single uncertainty realization, and the robust inequalities are used to prohibit violation of constraints even in the worst-case realization. To the best of our knowledge, the need for a heterogeneous framework that handles multi-scale uncertainties has not been addressed in the literature, which is the goal of this work.

General Modeling Framework

Deterministic model

Before introducing the proposed stochastic robust optimization model for supply chain design and operations under multi-scale uncertainties, we first present the corresponding deterministic model. A general form of the deterministic model is given below, based on which an uncertainty counterpart will be developed.

$$\begin{aligned} \min \quad & C^{str}(x,y)+C^{opr}(x,y,z) \\ \text{s.t.} \quad & Ax+By \geq d \\ & Ex+Fy+Gz \geq h \\ & x \in \{0,1\}^n, y \in \mathbb{R}^m, z \in \mathbb{R}^r \end{aligned} \tag{PD}$$

where x denotes the binary variables for strategic decisions, which model the selection of locations for manufacturing facilities and warehouses; choice of manufacturing technologies, storage types, and transportation modes, etc.; y denotes the continuous variables for strategic decisions, which include the capacities of manufacturing facilities and warehouses; z represents the continuous operational decisions, which involve the quantities of raw materials to acquire from suppliers and products to sell to customers, target of production to reach, as well as amounts of materials to transfer through the transportation links and to hold in the inventory.

The deterministic model (PD) can be divided into two parts. The first part corresponds to supply chain design. $C^{str}(x,y)$ stands for the amortized capital cost associated only with strategic decisions. The inequality $Ax+By \geq d$ represents the strategic-level constraints, involving network design, capacity limits, as well as economic models for capital investment and fixed operating cost. The second part corresponds to supply chain operations. $C^{opr}(x,y,z)$ stands for the operational cost that is influenced by both strategic and operational decisions. The inequality $Ex+Fy+Gz \geq h$ represents the operational level constraints, covering material balances, bounding constraints, and cost calculations of various supply chain activities. Although model (PD) is formulated as a minimization problem, it can be easily generalized to maximize other economic indicators (e.g., net present value and return on investment) by minimizing the negative.

Problem (PD) is often formulated as a mixed-integer linear programming (MILP) model for optimal supply chain design and planning. If all parameters are known and fixed, the deterministic model (PD) can then be employed to optimize the economic performance of supply chains.

Stochastic robust optimization model

When supply chain design decisions must be made before the realization of uncertain parameters, two-stage optimization models are often employed.[6,56] In such models, the first-stage (strategic) decisions are made "here-and-now" before realization of any uncertainty, and the second-stage (operational) decisions are made in a "wait-and-see" manner after all uncertainties are revealed. Instead of handling all types of uncertainty with a uniform approach, we handle strategic and operational uncertainties differently and reflect the decision maker's different levels of conservativeness with the following stochastic robust optimization model.

$$\begin{aligned} \min \quad & C^{str}(x,y)+E_{\omega\in\Omega}\left[\overline{C}_{\omega}^{opr}(x,y)\right] \\ \text{s.t.} \quad & Ax+By \geq d \\ & x \in \{0,1\}^n, y \in \mathbb{R}^m \\ & \left\{ \begin{aligned} \overline{C}_{\omega}^{opr}(x,y)= \max_{u_\omega \in U_\omega} \min_{z} \quad & C_{\omega}^{opr}(x,y,z_\omega,u_\omega) \\ \text{s.t.} \quad & Gz_\omega \geq h_\omega - E_\omega x - F_\omega y - K_\omega u_\omega \\ & z_\omega \in \mathbb{R}^r \end{aligned} \right\}, \\ & \forall \omega \in \Omega \end{aligned} \tag{P0}$$

where ω denotes a particular realization of strategic uncertainties, and u_ω denotes a particular realization of operational uncertainties. As can be seen, the proposed model (P0) explicitly reflects the decision maker's different levels of conservativeness. An expectation over all strategic uncertainty realizations is considered in the objective function, showing that the decision maker is considering all possibilities. Conversely, the value of $\overline{C}_{\omega}^{opr}(x,y)$ represents the worst-case operationing cost under strategic uncertainty realization ω at given first-stage decisions according to the max–min problem. Therefore, the decision maker hedges against the worst-case realization of operational uncertainties defined by the uncertainty set U_ω in problem (P0). Please also note that the uncertainty set U_ω for operational uncertainties is indexed by realization ω of the strategic uncertainty. In this way, we allow the range of variation in operational uncertainties to be dependent on the realization of strategic uncertainties. This is critical as strategic uncertainties may have significant impacts on operational uncertainties.

As there can be infinite realizations of strategic uncertainties, the expectation function in (P0) is usually transformed approximately into a tractable optimization problem by introducing a finite number of scenarios. We name the resulting model a nested stochastic robust optimization model, because a robust optimization problem is nested in a two-stage stochastic program.

$$\begin{aligned} \min \quad & C^{str}(x,y)+\sum_{s\in S} p_s \overline{C}_{s}^{opr}(x,y) \\ \text{s.t.} \quad & Ax+By \geq d \\ & x \in \{0,1\}^n, y \in \mathbb{R}^m \\ & \left\{ \begin{aligned} \overline{C}_{s}^{opr}(x,y)= \max_{u_s \in U_s} \min_{z} \quad & C_{s}^{opr}(x,y,z_s,u_s) \\ \text{s.t.} \quad & Gz_s \geq h_s - E_s x - F_s y - K_s u_s \\ & z_s \in \mathbb{R}^r \end{aligned} \right\}, \\ & \forall s \in S \end{aligned} \tag{P1}$$

where the index ω in (P0) is replaced by scenario s. The expectation function is replaced by the summation over all scenarios, where p_s denotes the probability of scenario s of strategic uncertainty realization. This is relevant when we have a number of long-term projections at hand (e.g., good, normal, and bad scenarios for the future climate) or we have a good estimate of the distribution of the strategic uncertainties (e.g., process conversion efficiency from historical data).

Without loss of generality, model (P1) can also be extended for risk management of strategic uncertainties by incorporating appropriate risk measures into the stochastic programming model.

The proposed stochastic robust optimization model (P1) is a multi-level MILP. Due to the existence of min–max–min function, problem (P1) cannot be solved directly by any off-the-shelf solver. Therefore, we introduce a tailored solution strategy in the next section for its solution.

Solution Strategy

To solve problem (P1), we take advantage of the C&CG algorithm that was recently shown to be efficient in solving two-stage robust optimization problems.[8] To demonstrate the algorithm, we first transform the multi-level MILP (P1) into an equivalent single-level MILP. We then describe how the problem can be decomposed into a master problem and a series of subproblems. The C&CG algorithm is implemented to solve the master and subproblems iteratively until a solution within the optimality tolerance is obtained.

It can be shown that the value of uncertain parameters at the optimal solution will be at one of the extreme points of the uncertainty set. Therefore, if we enumerate all the extreme points, then problem (P1) can be reduced to an equivalent (probably large-scale) MILP by removing the max–min function. Specifically, we can replace the content in the curly bracket in problem (P1) with the following.

$$\left\{\begin{array}{l}\overline{C}_s^{opr}(x,y) \geq C_{s,l}^{opr}\left(x,y,z_{s,l}\right)\\ Gz_{s,l} \geq h_s - E_s x - F_s y - K_s u_{s,l}\\ z_s \in \mathbb{R}^r\end{array}\right\}, \forall l \in L \qquad \text{(EP)}$$

where $u_{s,l}$ denotes an extreme point of the uncertainty set U_s.

However, a critical issue is that when the number of extreme points is very large the equivalent problem might be computationally intractable due to the size. Consequently, we decompose the problem based on the idea of partial enumeration, and obtain a master problem that has the same structure as the equivalent MILP but contains only a subset of the extreme points. Thus, the master problem constitutes a valid relaxation and provides a lower bound. To obtain upper bounds and feasible solutions, we solve a series of max–min operational-level subproblems at given first-stage decisions and strategic uncertainty realization s. Note that a max–min subproblem is developed for each scenario, which is different from the single subproblem in the original C&CG algorithm.[8] It can be proved that a set of new extreme points would be generated in each iteration if the termination criterion is not met.[8] Based on these extreme points, we can add an optimality cut to the master problem at the end of each iteration, thus enhancing the relaxation and generating a sequence of non-decreasing lower bounds. The optimality cut would be in the form of (EP) but corresponds only to one new extreme point. General formulations of the master problem (MP) and subproblems (SP) are given in Appendix A. Implementation of the improved C&CG algorithm is provided by the pseudo code below.

Algorithm. Column-and-constraint generation (C&CG) algorithm

Step 1 (Initialization)

Set $LB \leftarrow -\infty$, $UB \leftarrow +\infty$, $l \leftarrow 0$, $\underline{L} \leftarrow \varnothing$, and $\xi \leftarrow 10^{-3}$.

Step 2 (Lower Bounding)

Solve the master problem (MP).

Denote the optimal solution as $\left(x^{*(l+1)}, y^{*(l+1)}, \overline{C}_s^{*opr(l+1)}, z_{s,l}^{*(l+1)}\right)$.

Set $LB \leftarrow C^{str}\left(x^{*(l+1)}, y^{*(l+1)}\right) + \sum_{s\in S} p_s \overline{C}_s^{*opr(l+1)}$

Step 3 (Upper Bounding)

for $s \in S$

  Solve the subproblem (SP) corresponding to scenario s at $\left(x^{*(l+1)}, y^{*(l+1)}\right)$.

  Denote the optimal solution as $\left(\hat{z}_s^{(l+1)}, \hat{u}_s^{(l+1)}\right)$.

end

Set $UB \leftarrow \min\left\{UB, \left[C^{str}\left(x^{*(l+1)}, y^{*(l+1)}\right) + \sum_s p_s C_s^{opr}\left(x^{*(l+1)}, y^{*(l+1)}, \hat{z}_s^{(l+1)}, \hat{u}_s^{(l+1)}\right)\right]\right\}$

Step 4 (Loop)

if $\left|\frac{UB-LB}{UB}\right| < \xi$, **then**

  Terminate and return the optimal solution.

else

  Generate an optimality cut corresponding to $\hat{u}_s^{(l+1)}$ and add it to (MP).

  Set $\underline{L} \leftarrow \underline{L} \cup \{l+1\}$ and $l \leftarrow l+1$.

  Go to step 2

end

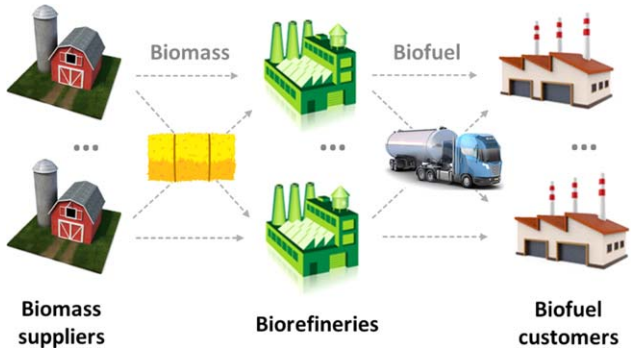

Figure 2. Superstructure of a three-echelon biomass-to-biofuel supply chain.

[Color figure can be viewed in the online issue, which is available at wileyonlinelibrary.com.]

Case Study

Case definition and model formulation

To demonstrate the applicability of the proposed modeling framework and solution algorithm, we consider an application on the optimal design and operations of a potential biofuel supply chain in Illinois. Largely driven by the societal concerns on climate change, energy security and the non-renewable nature of fossil fuels, production of biofuels soared in the past decade.[57] As the biofuel technologies related to production and logistics are maturing, the design and operations of the supply chain are now recognized as significant factors influencing the economic performances of a biofuel supply chain.[58]

Mathematical programming and process systems engineering tools have been extensively employed for biofuel and bioenergy supply chain optimization.[5,59–61] Most early models were formulated as deterministic MILPs with spatially explicit, multi-echelon, and multi-period features.[61–66] To address the questions on how green or how sustainable a biofuel supply chain is, multi-objective models have been proposed to include environmental sustainability criteria in addition to the traditional economic metrics.[58,67–72] Recently, a number of game-theory models were developed that view biofuel supply chains from a decentralized perspective and account for multiple players in the market.[73–76] To hedge against uncertainties in supply chain design and operations, models using various methods for optimization under uncertainty can be found in the literature, which cover a wide spectrum of pricing and quantity uncertainties in biofuel supply chains.[21,77,78]

Following the proposed stochastic robust optimization approach, we modify the deterministic spatially explicit and multi-period MILP model developed by You et al.[58] to handle strategic and operational uncertainties in a biofuel supply chain. The underlying three-echelon supply chain superstructure is shown in Figure 2, including a set of biomass suppliers, a set of candidate sites for building biorefineries, and a set of biofuel customers. In this case study, the biomass feedstock is corn stover, and the biofuel product is fuel ethanol. The biomass-to-biofuel conversion is via a bio-chemical pathway.[79] The supply chain optimization is performed at the county level in Illinois. We consider 25 counties with the highest annual yield of corn stover as the potential biomass suppliers, 40 counties with the highest annual demand of fuel ethanol as the potential biofuel customers, and 10 counties with moderate biomass yield and biofuel demand as the candidate sites for building biorefineries. Three capacity levels of ethanol production at biorefineries are considered, namely 10–50, 50–100, and 100–150 MM gallons/year. A minimum capacity of 10 MM gallons/year is imposed if a biorefinery is built. To account for the seasonality in biomass supply, we employ a monthly-based multi-period model. We assume that corn stover can only be harvested in October and November.[80] The first-stage decisions include the selection of location and determination of capacity for biorefineries, which must be made before the realization of both strategic and operational uncertainties. The second-stage decisions involve the various continuous variables on biomass acquisition, biofuel sales, inter-site transportation, and inventory management. These second-stage decisions are made after the realization of both strategic and operational uncertainties. Complete recourse is assumed by allowing the use of imported biofuel from an external source to satisfy the unmet demand. However, a penalty cost is imposed for using imported biofuel.

The objective is to minimize the expected total cost over different scenarios of strategic uncertainty realization while ensuring the robustness against operational uncertainties. The strategic uncertainties considered in this case study include technology evolution and climate and weather. Uncertainty in technology evolution is reflected as the deviation of actual process conversion efficiency from the designated value, which may originate from design or implementation errors. Uncertainty of climate and weather is reflected in the variations of precipitation and insolation, which greatly impact the yield of biomass feedstock. The operational uncertainties include variations in biomass supply and biofuel demand. Details on the modeling of these uncertain parameters are summarized in Table 1. We consider three scenarios for the uncertain conversion efficiency which are equal to 90, 100, and 110% of the nominal value, respectively. We also consider three scenarios for the influence of climate and weather, representing good, normal and bad years, respectively. Therefore, we have a total of 9 ($=3\times3$) scenarios for strategic uncertainties. We choose nine scenarios in this case study for ease of exposition. Without loss of generality, the proposed modeling framework and solution algorithm can account for more scenarios if more information regarding the strategic uncertainties is available (e.g., prediction from historical data). It is worth noting that the range of variation in biomass availability differs in different climate and weather scenarios. This relationship reflects the dependency of operational uncertainty in biomass supply on the strategic uncertainty in climate and weather. The other operational uncertainty, demand fluctuation, is independent of the strategic uncertainties. Therefore, its corresponding uncertainty set is the same for all scenarios. The nominal values for these uncertainties as well as other model parameters are obtained from the literature and various public sources.[58,80–85]

Following the proposed stochastic robust optimization approach and the C&CG algorithm, we construct the master and subproblem, which are presented in Appendix B. The master problem involves Eqs. (B1)–(B17), and the subproblem involves Eqs. (B18)–(B35). Both master and subproblem are formulated as MILPs. Therefore, the C&CG algorithm requires only an MILP solver.

Comparison with traditional approaches

The stochastic robust optimal solution under both strategic and operational uncertainties are shown in Figure 3a. The optimal first-stage decisions indicate that a total of six biorefineries should be built. The three biorefineries in Whiteside

Table 1. Scenarios and Bounded Uncertainty Sets of Strategic and Operational Uncertainties

		Strategic uncertainties		Operational uncertainties	
	Probability	Conversion efficiency	Climate and weather	Biomass availability	Biofuel demand
Deterministic		α	Normal	a	d
Scenario 1	1/12	0.9α			
Scenario 2	1/6	α	Bad	[0.7a, 0.9a]	
Scenario 3	1/12	1.1α			
Scenario 4	1/12	0.9α			
Scenario 5	1/6	α	Normal	[0.9a, 1.1a]	[0.9d, 1.1d]
Scenario 6	1/12	1.1α			
Scenario 7	1/12	0.9α			
Scenario 8	1/6	α	Good	[1.1a, 1.3a]	
Scenario 9	1/12	1.1α			

County, McLean County and Champaign County are all at the maximum capacity of 150 MM gallons/year. Besides, there are three small-scale biorefineries built in LaSalle County, Kankakee County, and Sangamon County with the capacity of 10, 13, and 17 MM gallons/year. For comparison, we also solve a deterministic MILP by setting the process conversion efficiency, biomass availability, and biofuel demand at the nominal values. The resulting supply chain layout is given in Figure 3b. Two biorefineries are built in Whiteside County and McLean County at the maximum capacity of 150 MM gallons/year, and another biorefinery is built in Champaign County at the capacity of 145 MM gallons/year. Comparing Figures 3a, 3b, we can observe that majority of the demands is satisfied by the three large-scale biorefineries. The other three biorefineries built in Figure 3a hedge against the variations in biomass availability and biofuel demand. These additional ethanol production capacities can be utilized when biofuel demands are higher than the nominal values. Viewed from another perspective, the distribution of these three biorefineries make it easier to acquire biomass from more suppliers when the biomass availabilities are lower than the nominal values. To compare with the solutions from a uniform modeling approach, we also solve the problem using a standard two-stage stochastic programming approach. To replace the corresponding uncertainty sets used in the nested stochastic robust optimization model, we sample 30 scenarios for the uncertain biomass availability and biofuel demand at all suppliers and customers through the Monte Carlo method within the bounds in Table 1. According to a standard approach for calculating the confidence interval,[52] with 30 scenarios for the operational uncertainties, the interval between $\pm 1\%$ of the calculated expectation corresponds to a 95% confidence level. In addition, we still have three scenarios for the uncertain conversion efficiency. Consequently, we employ a total of 90 ($=3 \times 30$) scenarios to formulate a standard two-stage stochastic program without max–min functions. The resulting supply chain layout is shown in Figure 3c. Besides the three maximum-capacity biorefineries in Whiteside County, McLean County, and Champaign County, a biorefinery of 11 MM gallons/year is built in Kankakee County. As can be observed, the stochastic programming solution is like a compromise solution between the stochastic robust solution and the deterministic solution.

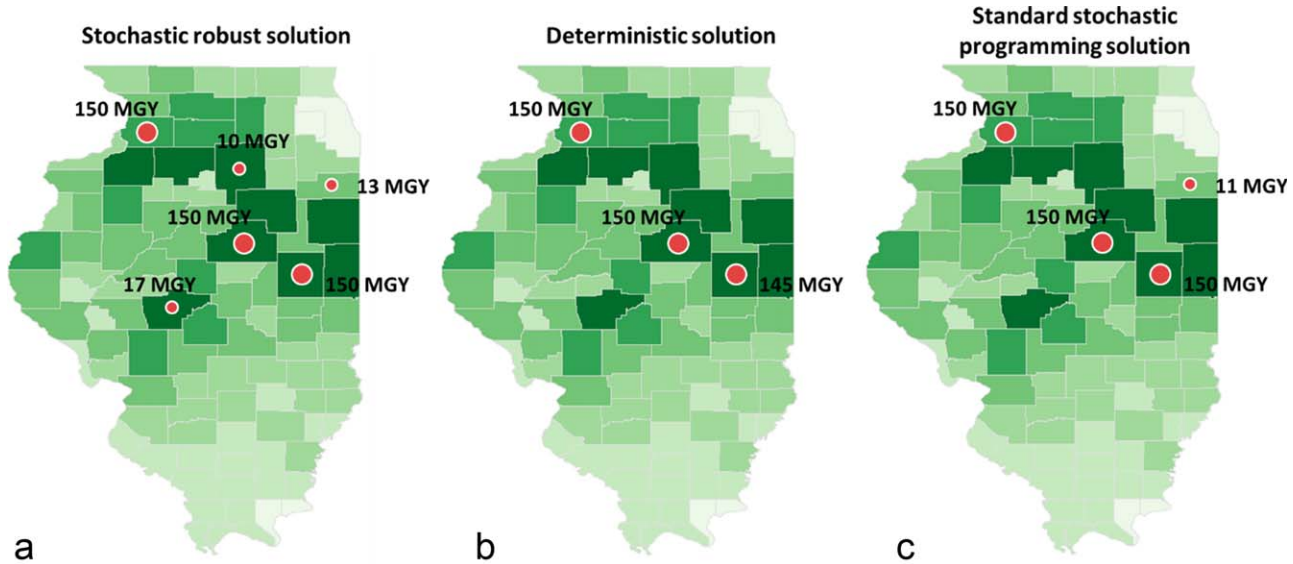

Figure 3. Optimal supply chain layout from the (a) stochastic robust solution, (b) deterministic solution, and (c) standard stochastic programming solution.

The backgrounds represent the nominal biomass availability across Illinois. [Color figure can be viewed in the online issue, which is available at wileyonlinelibrary.com.]

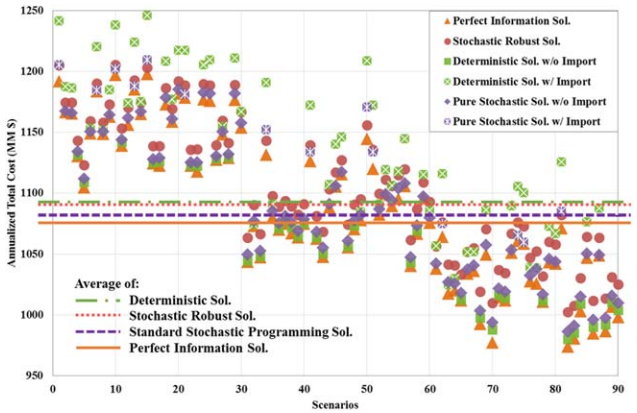

Figure 4. Simulation results for different supply chain designs in randomly generated 90 scenarios.

[Color figure can be viewed in the online issue, which is available at wileyonlinelibrary.com.]

To demonstrate the performances of all three supply chain designs in an uncertain environment, we perform a simulation in all the aforementioned 90 scenarios for each supply chain design. The results are plotted in Figure 4, where the X-axis represents the index of scenarios and the Y-axis represents the annualized total cost. The orange triangles denote the perfect information solutions, which are obtained by solving a deterministic model for each scenario that optimizes both strategic and operational decisions. These perfect information solutions indicate the best economic performance one can achieve in each scenario. The red circles denote the stochastic robust solutions corresponding to Figure 3a. We observe that the supply chain design given by the stochastic robust optimization approach does not require biofuel import from the external source in any of the scenarios. Therefore, 100% of the customer demands are satisfied within the state. The green squares denote the deterministic solutions corresponding to Figure 3b, among which the crossed green squares indicate that ethanol import from the external source are needed in 55 out of the 90 scenarios. That is to say, merely 39% of the demands are satisfied within the state. The purple diamonds denote the standard stochastic programming solutions corresponding to Figure 3c, among which the crossed purple diamonds indicate that ethanol import from the external source are needed in 14 out of the 90 scenarios, so that 84% of the demands can be satisfied by this supply chain design. We also plot the expected total costs over all the 90 scenarios for each supply chain design in Figure 4, as given by the horizontal lines at the center. Apparently, the perfect information solutions set the baseline. The expected cost of the stochastic robust solution is higher than that of the stochastic programming solution. The difference of about $10 MM can be considered to be the cost for improving the demand fulfill rate from 84 to 100%. Although easier to obtain, the deterministic solution has an expected cost that is even slightly higher than the stochastic robust solution. This indicates that deterministic supply chain optimization at nominal values without considering uncertainties explicitly can lead to lower demand fulfill rate and higher expected total cost.

Cost and inventory profiles

To take a close look at the stochastic robust solution, we present its cost breakdown and inventory profile in the scenario where all uncertain parameters are set to their nominal values. Note that the various costs for energy, utility, chemicals, wages, etc. are grouped by supply chain activities, as shown by Figure 5. The largest cost comes from capital investment for building the biorefineries, which accounts for 30%. The second largest cost is from biomass acquisition accounting for 20% of the total cost. This indicates that the purchase price of biomass has a significant impact on the total cost. The biomass-related logistics costs are also considerable. The biomass inventory holding cost accounts for 14% of the total cost. This is because corn stover can only be harvested in limited months and a large quantity of biomass must be carefully stored to minimize material degradation throughout the year. The biomass transportation cost accounts for 13% because the transportation density of corn stover is low and its supply is sparsely distributed across the state. In contrast, the biofuel-related logistics costs are much lower because ethanol has a higher density and is easier for storage.

To show the material flows within the supply chain network, we draw a Sankey diagram as shown in Figure 6. The nodes on the left, middle, and right represent the biomass suppliers, biorefineries, and biofuel customers, respectively. The links between suppliers and biorefineries denote the total transportation amounts of corn stover over all 12 months. The links between biorefineries and customers denote the total transportation amounts of ethanol over all 12 months. As can be seen, the three large-scale biorefineries consume the corn stover feedstock from multiple biomass suppliers, and the three small-scale biorefineries only utilize local biomass resources. Most biofuel customers are served by a single biorefinery, but the cook county is supplied by multiple biorefineries because of its high population density and high demand in transportation fuels. A total of 5893 ktons of corn stover is shipped from biomass suppliers to biorefineries. A total of 445 MM gallons of ethanol is shipped from biorefineries to biofuel customers, corresponding to 5638 ktons of corn stover being converted. The difference between the amounts of corn stover received and used at the biorefineries is due to the degradation of biomass in the inventory.

The monthly inventory profiles of corn stover and ethanol corresponding to the nominal scenario is shown in Figure 7. Each column represents the level of total corn stover inventory over all biorefineries in a certain month, and each circle represents the level of total ethanol inventory. Overall, the corn stover inventory accumulates in October and November, which

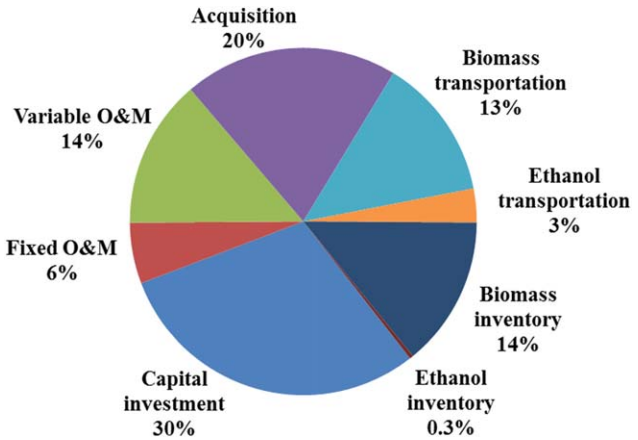

Figure 5. Cost break down of the stochastic robust solution in the nominal scenario.

[Color figure can be viewed in the online issue, which is available at wileyonlinelibrary.com.]

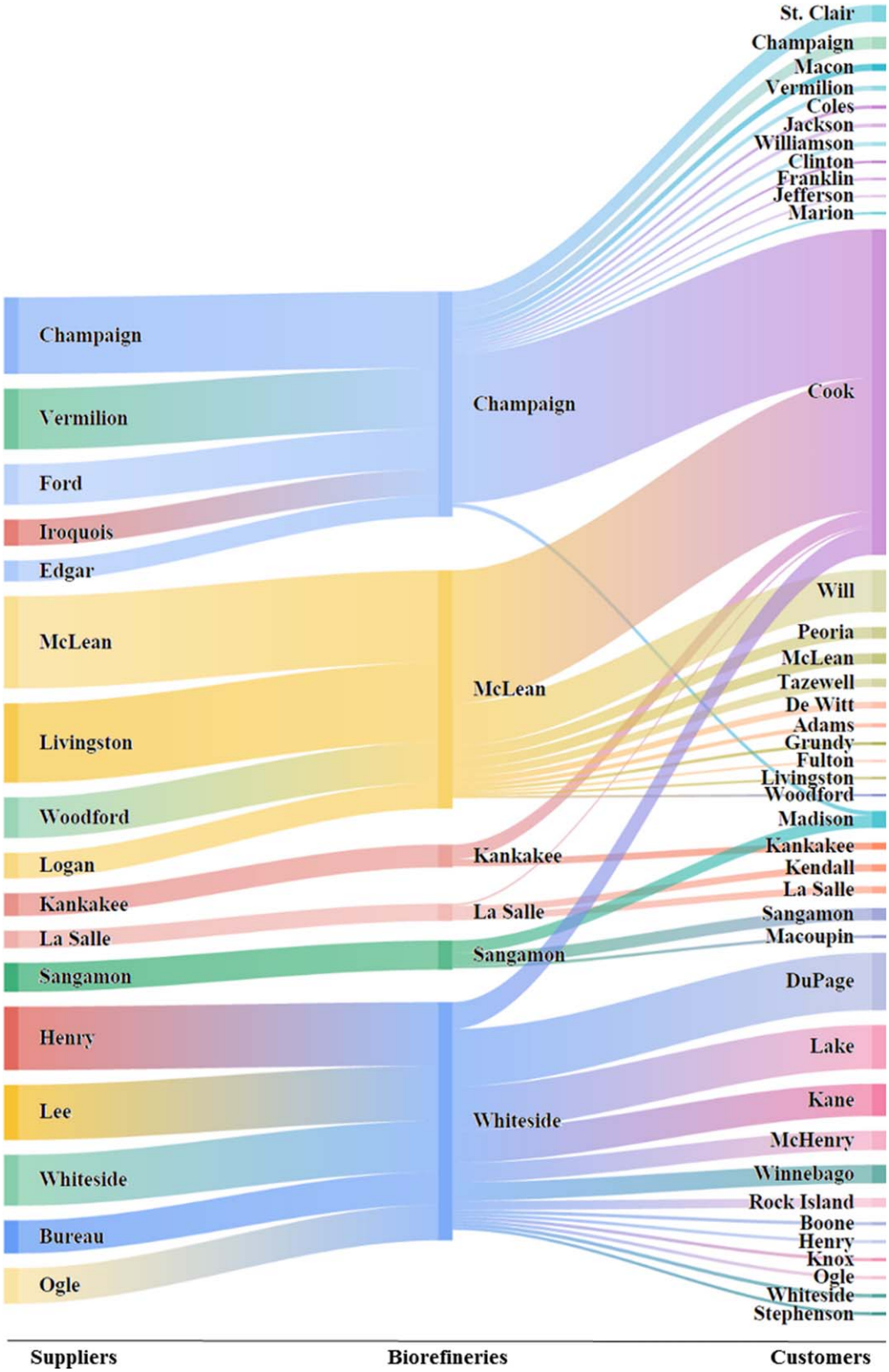

Figure 6. Flows of corn stover and fuel ethanol within the supply chain network.

[Color figure can be viewed in the online issue, which is available at wileyonlinelibrary.com.]

are the only season that corn stover can be harvested. The corn stover inventory is then carried in biorefineries throughout the year for production of biofuels. Conversely, the ethanol inventory climbs since October, and reaches its peak in July. As can be seen, ethanol production almost stops in September. Specifically, the three large-scale biorefineries have shut down their processes and merely use ethanol inventory to satisfy the demands in September. The direct cause is that almost all the stocked corn stover has been converted into ethanol in August. The rationale behind this phenomenon is that the biorefineries

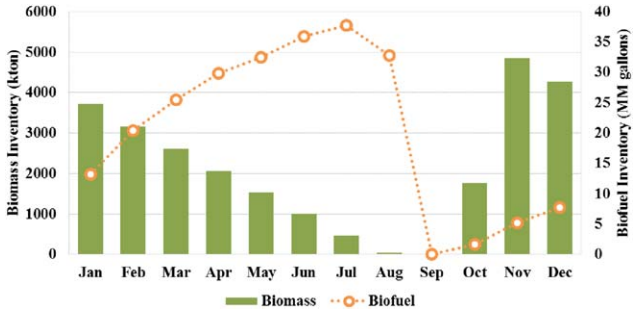

Figure 7. Inventory profile of the stochastic robust solution in the nominal scenario.

[Color figure can be viewed in the online issue, which is available at wileyonlinelibrary.com.]

tend to convert biomass into biofuel as soon as possible to avoid the high biomass inventory cost and degradation of biomass. Since the stochastic robust solution has a higher annual production capacity than the nominal demand, the biorefineries have the capability to consume all corn stover in less than 12 months.

Uncertainty budgets

The classical worst-case solution of robust optimization has been criticized by its over-conservativeness. Therefore, to add the flexibility in controlling the conservativeness of the resulting robust operational solution, we also consider the constraints of budget uncertainty when defining the uncertainty sets.[7] In this case study, we have two types of uncertainty budgets. The first type of budget is for uncertain biomass availability over all biomass suppliers. If set at an integer value, it reflects the number of biomass suppliers whose biomass availability may deviate. The second type of budget is for uncertain biofuel demand over all biofuel customers. If set at an integer value, it reflects the number of biofuel customers whose biofuel demand could deviate. By setting the two types of uncertainty budgets at different values between their lower and upper bounds, we obtain the solution profile in Figure 8, where the X-axis represents the uncertainty budget for biofuel demand, the Y-axis represents the uncertainty budget for biomass availability. The number in each cell represents the objective value of the stochastic robust solution at the corresponding combination of uncertainty budgets. From green to yellow and to red, we color the cells based on the numbers inside, from the lowest expected cost of \$973 MM to the highest expected cost of \$1208 MM. According to the horizontal color scale at the bottom of Figure 8, the solutions toward the upper left corner have a lower cost and tend to be less conservative, whereas the solutions toward the lower right corner have a higher cost and tend to be more conservative. This trend clearly suggests that the more robust a solution is against operational uncertainties, the higher its cost will be. Note that the aforementioned stochastic robust solution corresponds to the cell in the lower right corner, of which both budgets are at their maximum. Viewing by rows, we can observe a sharp increase in total cost when the biofuel demand budget switches from 0 to 20% of the maximum budget. The total cost then climbs gradually as the biofuel demand budget increases from 20 to 100%. This is because the demands of certain counties are significantly larger than that of the other counties. Demand variations of the counties with higher demands are handled first, and that of the counties with lower demands are handled later when the biofuel demand budget increases. Viewing by columns, we can see that the total cost climbs gradually as the uncertainty budget for biomass availability increases. This indicates that the impact of biomass availability budget might not be as significant as that of the biofuel demand budget.

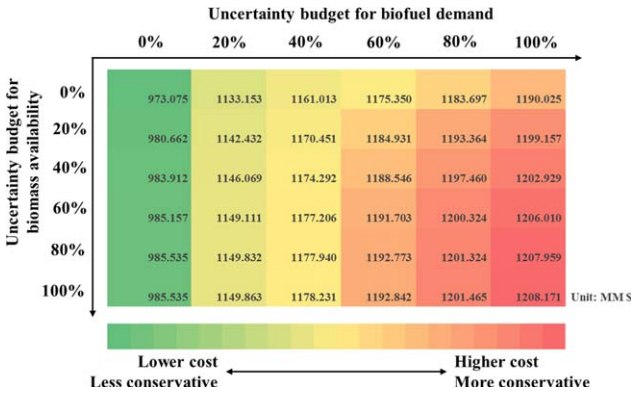

Figure 8. Solution profile across the uncertainty budget table.

[Color figure can be viewed in the online issue, which is available at wileyonlinelibrary.com.]

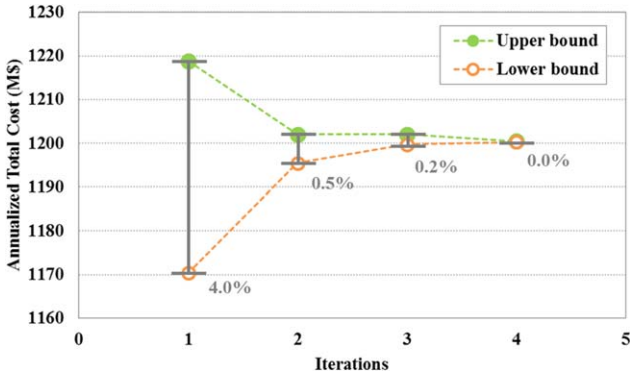

Figure 9. Upper and lower bounds of the C&CG algorithm in each iteration.

[Color figure can be viewed in the online issue, which is available at wileyonlinelibrary.com.]

We note that similar flexibility may also be achieved by considering appropriate risk management metrics or changing the number and weights of scenarios in stochastic programming. However, using robust optimization approach for operational uncertainties is considered more advantageous from the following prospects.[28] First, the worst-case scenario may not always be straightforward to identify. Second, construction of uncertainty sets in the robust optimization does not require information on probability distribution, which is essential for stochastic programming. Third, the robust counterpart problem is computationally more tractable, and stochastic programming is known for its curse of dimensionality.[86]

Computational performances

We solve the MILP master problem with CPLEX 12, and we solve the subproblem based on the strong duality, of which the resulting MILP is also solved with CPLEX 12. All computational experiments are carried out on a PC with an Intel Core i5-2400 CPU at 3.10 GHz and 8.00 GB RAM. All models and solution procedures are coded in GAMS 24.5.6.[87] The optimality tolerance for CPLEX 12 is set to 0. The relative tolerance ξ for the C&CG algorithm is set to 0.1%.

As aforementioned, the C&CG algorithm involves iterative solution of one master problem and multiple subproblems.

The subproblem in all iterations has 65 binary variables, 2161 continuous variables, and 11,103 constraints. The master problem in the first iteration has 30 binary variables, 63,421 continuous variables, and 19,551 constraints. As the algorithm iterates, the size of the master problem increases because an optimality cut is added at the end of each iteration. Among the 36 instances shown in Figure 5, the minimum number of iterations is 1, and the maximum number of iterations is 8. The master problem at the 8th iteration has 30 binary variables, 506,941 continuous variables, and 155,694 constraints. The shortest solution time is 117 CPU seconds, while the longest solution time is about 14.5 CPU hours. To give a glance at the computational performance of the C&CG algorithm, we select one instance that involves multiple iterations and present its solution process in Figure 9. This instance corresponds to the biomass availability budget of 60% and the biofuel demand budget of 80%. The X-axis is the number of iterations, and the Y-axis is the objective value. As can be seen, the algorithm converges in four iterations, and the relative gap falls within 1% at the second iteration. Overall, the C&CG is shown to be capable of achieving a small relative optimality gap in its early iterations and converge within a reasonable number of iterations and solution time.

Conclusion

A nested stochastic robust optimization model was proposed to handle both strategic and operational supply chain uncertainties in a holistic framework. Considering the cases that a decision maker is less conservative toward strategic uncertainties and more conservative toward operational uncertainties, we modeled the multi-scale uncertainties via integration of stochastic programming and robust optimization approaches. Potential dependency of the operational uncertainties on strategic uncertainties was explicitly handled in the proposed model. The resulting formulation was a multi-level MILP involving expectation over multiple scenarios as well as max–min problems that guarantee the robustness of operations. We employed a decomposition-based C&CG algorithm for the solution, which was based on partial enumeration and a single master problem and multiple subproblems. The application was demonstrated by a county-level case study on optimal design of a spatially-explicit biofuel supply chain in Illinois. The optimal supply chain configuration derived from the stochastic robust optimization approach was compared with those from the deterministic model and standard two-stage stochastic programming approach. Demand fulfill rate of the stochastic robust solution is 16% higher than that of the standard stochastic programming solution and 61% higher than that of the deterministic model solution. The flexibility in controlling the conservativeness of the resulting stochastic robust solution was also illustrated by adjusting two uncertainty budgets from 0 to 100%. Regarding the computational performances, the C&CG algorithm was able to solve all instances of the resulting multi-level MILP in no more than eight iterations with reasonable amount of time.

Acknowledgment

The authors acknowledge financial support from the Institute for Sustainability and Energy at Northwestern University (ISEN) and the National Science Foundation (NSF) CAREER Award (CBET-1554424).

Notation

All sets, parameters, and parameters employed in the stochastic robust optimization model are summarized below. As a convention, all parameters are denoted in lower-case symbols or Greek letters, and all variables are denoted with a capitalized first letter.

Sets/Indices

G = Set of technologies indexed by g
I = Set of suppliers indexed by i
J = Set of biorefineries indexed by j
K = Set of customers indexed by k
L = Set of extreme points indexed by l
R = Set of capacity levels indexed by r
S = Set of scenarios indexed by s

Parameters

$\hat{a}_{b,i,t,s,l}$ = availability of biomass b at supplier i in time period t in scenario s at extreme point l
$\underline{a}_{b,i,t}$ = basic availability for biomass b at supplier i in time period t
$\hat{a}_{b,i,t}$ = maximum deviation of availability for biomass b at supplier i in time period t
ann = annuity
$capx_{j,g}$ = capacity of biorefinery j with technology g
cf_g = ratio of fixed operations and maintenance cost to capital cost for technology g
$cim_{p,k,t}$ = importing cost for biofuel p to customer k in time period t
$cm_{p,j,t,g}$ = variable operations and maintenance cost for producing biofuel p in biorefinery j in time period t with technology g
$cr_{j,r,g}$ = reference capital cost of biorefinery j at capacity level r with technology g
$ctb_{b,i,j}$ = transportation cost for shipping biomass b from supplier i to biorefinery j
$ctp_{p,j,k}$ = transportation cost for shipping biofuel p from biorefinery j to customer k
$\hat{d}_{p,k,t,s,l}$ = level of demand for biofuel p at customer k in time period t in scenario s at extreme point l
$\underline{d}_{p,k,t}$ = basic demand for biofuel p at customer k in time period t
$\hat{d}_{p,k,t}$ = maximum deviation of availability for biofuel p at customer k in time period t
h_t = length of time period t
$hb_{b,j,t}$ = inventory cost for holding biomass b in biorefinery j in time period t
$hp_{p,j,t}$ = inventory cost for holding biofuel p in biorefinery j in time period t
mcb_b = water content of biomass b
$pcc_{b,i,t}$ = acquisition cost for biomass b at supplier i in time period t
prb_s = probability of scenario s
$pr_{j,r,g}$ = bound of biorefinery j at capacity level r with technology g
rt = length of a year
$\widehat{\alpha}_{b,p,s,g}$ = efficiency for converting biomass b to biofuel p with technology g in scenario s
$\beta_{b,p,g}$ = efficiency for converting biomass b into biofuel p with technology g
Γa_b = budget uncertainty for biomass b
Γd_p = budget uncertainty for biofuel p
η_j = minimum utilization rate of biorefinery j
φ_p = unit conversion factor for biofuel p
$\psi_{b,j,t}$ = loss of biomass b in biorefinery j in time period t

Continuous Variables

$Cp_{j,r,g}$ = capacity of biorefinery j at capacity level r with technology g
$D^{av}_{b,i,t}, D^{cpl}_{j,t,g}, D^{cpu}_{j,t,g}, D^{im}_{p,k,t}, D^{bm}_{b,j,t}, D^{con}_{p,j,t,g}, D^{pm}_{p,j,t}$ = dual variables
$Ep_{p,k,t,s,l}$ = amount of biofuel p imported to customer k in time period t in scenario s at extreme point l
$Fb_{b,i,j,t,s,l}$ = amount of biomass b shipped from supplier i to biorefinery j in time period t in scenario s at extreme point l
$Fp_{p,j,k,t,s,l}$ = amount of biofuel p shipped from biorefinery j to customer k in time period t in scenario s at extreme point l

$Gad^{av}_{b,i,t}$ = auxiliary variable for availability of biomass b at supplier i in time period t
$Gdd^{im}_{p,k,t}$ = auxiliary variable for demand of biofuel p at customer k in time period t
$Pb_{b,i,t,s,l}$ = amount of biomass b purchased at supplier i in time period t in scenario s at extreme point l
$Sb_{b,j,t,s,l}$ = inventory level of biomass b in biorefinery j in time period t in scenario s at extreme point l
$Sp_{p,j,t,s,l}$ = inventory level of biofuel p in biorefinery j in time period t in scenario s at extreme point l
$Wp_{p,j,t,s,g,l}$ = amount of biofuel p produced at biorefinery j in time period t in scenario s with technology g at extreme point l

Binary Variables

$Ga_{b,i}$ = level of deviation of availability for biomass b at supplier i
$Gd_{p,k}$ = level of deviation of demand for biofuel p at customer k
$X_{j,r,g}$ = 1 if biorefinery j at capacity level r with technology g is built; 0 otherwise

Literature Cited

1. Grossmann I. Enterprise-wide optimization: a new frontier in process systems engineering. *AIChE J*. 2005;51(7):1846–1857.
2. Shah N. Pharmaceutical supply chains: key issues and strategies for optimisation. *Comp Chem Eng*. 2004;28(6–7):929–941.
3. Garcia DJ, You F. Supply chain design and optimization: challenges and opportunities. *Comp Chem Eng*. 2015;81:153–170.
4. Sahinidis NV. Optimization under uncertainty: state-of-the-art and opportunities. *Comp Chem Eng*. 2004;28(6–7):971–983.
5. Yue D, You F, Snyder SW. Biomass-to-bioenergy and biofuel supply chain optimization: overview, key issues and challenges. *Comp Chem Eng*. 2014;66:36–56.
6. Birge JR, Louveaux F. *Introduction to Stochastic Programming*. New York: Springer Science & Business Media, 2011.
7. Bertsimas D, Sim M. The price of robustness. *Operat Res*. 2004; 52(1):35–53.
8. Zeng B, Zhao L. Solving two-stage robust optimization problems using a column-and-constraint generation method. *Operat Res Lett*. 2013;41(5):457–461.
9. Barbaro A, Bagajewicz MJ. Managing financial risk in planning under uncertainty. *AIChE J*. 2004;50(5):963–989.
10. Applequist GE, Pekny JF, Reklaitis GV. Risk and uncertainty in managing chemical manufacturing supply chains. *Comp Chem Eng*. 2000;24(9–10):2211–2222.
11. Papageorgiou LG. Supply chain optimisation for the process industries: advances and opportunities. *Comp Chem Eng*. 2009;33(12): 1931–1938.
12. Birge JR. State-of-the-art-survey—stochastic programming: computation and applications. *INFORMS J Comp*. 1997;9(2):111–133.
13. You F, Grossmann IE. Multicut Benders decomposition algorithm for process supply chain planning under uncertainty. *Annal Operat Res*. 2011;210(1):191–211.
14. Oliveira F, Grossmann IE, Hamacher S. Accelerating benders stochastic decomposition for the optimization under uncertainty of the petroleum product supply chain. *Comp Operat Res*. 2014;49:47–58.
15. Levis AA, Papageorgiou LG. A hierarchical solution approach for multi-site capacity planning under uncertainty in the pharmaceutical industry. *Comp Chem Eng*. 2004;28(5):707–725.
16. Tsiakis P, Shah N, Pantelides CC. Design of multi-echelon supply chain networks under demand uncertainty. *Ind Eng Chem Res*. 2001; 40(16):3585–3604.
17. Tong K, Gong J, Yue D, You F. Stochastic programming approach to optimal design and operations of integrated hydrocarbon biofuel and petroleum supply chains. *ACS Sustain Chem Eng*. 2014;2(1):49–61.
18. Shapiro A. Stochastic programming by Monte Carlo simulation methods. *Stochast Prog E Print Ser*. 2000:03.
19. Shapiro A, Homem-de-Mello T. A simulation-based approach to two-stage stochastic programming with recourse. *Math Prog*. 1998; 81(3):301–325.
20. Santoso T, Ahmed S, Goetschalckx M, Shapiro A. A stochastic programming approach for supply chain network design under uncertainty. *Europ J Operat Res*. 2005;167(1):96–115.
21. Gebreslassie BH, Yao Y, You F. Design under uncertainty of hydrocarbon biorefinery supply chains: multiobjective stochastic programming models, decomposition algorithm, and a comparison between CVaR and downside risk. *AIChE J*. 2012;58(7):2155–2179.
22. Gao J, You F. Deciphering and handling uncertainty in shale gas supply chain design and optimization: novel modeling framework and computationally efficient solution algorithm. *AIChE J*. 2015; 61(11):3739–3755.
23. Charnes A, Cooper WW. Chance-constrained Programming. *Manag Sci*. 1959;6(1):73–79.
24. Uryasev SP. *Probabilistic Constrained Optimization: Methodology and Applications*. Dordrecht: Springer, 2000.
25. Gupta A, Maranas CD, McDonald CM. Mid-term supply chain planning under demand uncertainty: customer demand satisfaction and inventory management. *Comp Chem Eng*. 2000;24(12):2613–2621.
26. Mitra K, Gudi RD, Patwardhan SC, Sardar G. Midterm supply chain planning under uncertainty: a multiobjective chance constrained programming framework. *Ind Eng Chem Res*. 2008;47(15):5501–5511.
27. Guillén-Gosálbez G, Grossmann I. A global optimization strategy for the environmentally conscious design of chemical supply chains under uncertainty in the damage assessment model. *Comp Chem Eng*. 2010;34(1):42–58.
28. Ben-Tal A, Nemirovski A. Robust optimization—methodology and applications. *Math Prog*. 2002;92(3):453–480.
29. Bertsimas D, Brown DB, Caramanis C. Theory and applications of robust optimization. *SIAM Rev*. 2011;53(3):464–501.
30. Pan F, Nagi R. Robust supply chain design under uncertain demand in agile manufacturing. *Comp Operat Res*. 2010;37(4):668–683.
31. Tong K, You F, Rong G. Robust design and operations of hydrocarbon biofuel supply chain integrating with existing petroleum refineries considering unit cost objective. *Comp Chem Eng*. 2014;68:128–139.
32. Ben-Tal A, Golany B, Nemirovski A, Vial J-P. Retailer-supplier flexible commitments contracts: a robust optimization approach. *Manuf Service Operat Manag*. 2005;7(3):248–271.
33. Lim S. A joint optimal pricing and order quantity model under parameter uncertainty and its practical implementation. *Omega*. 2013;41(6):998–1007.
34. Bellman RE, Zadeh LA. Decision-making in a fuzzy environment. *Manag Sci*. 1970;17(4):B-141–B-164.
35. Zimmermann HJ. *Fuzzy Set Theory—and Its Applications*. Netherlands: Springer, 2001.
36. Tong K, Gleeson MJ, Rong G, You F. Optimal design of advanced drop-in hydrocarbon biofuel supply chain integrating with existing petroleum refineries under uncertainty. *Biomass Bioenerg*. 2014;60: 108–120.
37. Tay DHS, Ng DKS, Sammons NE, Eden MR. Fuzzy optimization approach for the synthesis of a sustainable integrated biorefinery. *Ind Eng Chem Res*. 2011;50(3):1652–1665.
38. Peidro D, Mula J, Poler R, Verdegay J-L. Fuzzy optimization for supply chain planning under supply, demand and process uncertainties. *Fuzzy Set Syst*. 2009;160(18):2640–2657.
39. Snyder LV, Daskin MS. Reliability models for facility location: the expected failure cost case. *Transport Sci*. 2005;39(3):400–416.
40. Cui T, Ouyang Y, Shen Z-JM. Reliable facility location design under the risk of disruptions. *Operat Res*. 2010;58(4-part-1):998–1011.
41. You F, Grossmann IE. Integrated multi-echelon supply chain design with inventories under uncertainty: MINLP models, computational strategies. *AIChE J*. 2010;56(2):419–440.
42. You F, Grossmann IE. Balancing responsiveness and economics in process supply chain design with multi-echelon stochastic inventory. *AIChE J*. 2011;57(1):178–192.
43. You F, Grossmann IE. Mixed-integer nonlinear programming models and algorithms for large-scale supply chain design with stochastic inventory management. *Ind Eng Chem Res*. 2008;47(20):7802–7817.
44. You F, Grossmann IE. Stochastic inventory management for tactical process planning under uncertainties: MINLP models and algorithms. *AIChE J*. 2011;57(5):1250–1277.
45. You F, Pinto JM, Grossmann IE, Megan L. Optimal distribution-inventory planning of industrial gases. II. MINLP models and algorithms for stochastic cases. *Ind Eng Chem Res*. 2011;50(5):2928–2945.
46. Yue D, You F. Planning and scheduling of flexible process networks under uncertainty with stochastic inventory: MINLP models and algorithm. *AIChE J*. 2013;59(5):1511–1532.
47. Eppen GD, Martin RK, Schrage L. A scenario approach to capacity planning. *Operat Res*. 1989;37(4):517–527.
48. Rockafellar RT, Uryasev S. Conditional value-at-risk for general loss distributions. *J Bank Finance*. 2002;26(7):1443–1471.
49. Uryasev S, Rockafellar RT. Conditional value-at-risk: optimization approach. In: Uryasev SP, Pardalos PM, eds. *Stochastic Optimization: Algorithms and Applications,* Dordrecht: Kluwer Academic Publishers, 2001;54:411–435.

50. Carneiro MC, Ribas GP, Hamacher S. Risk management in the oil supply chain: a CVaR approach. *Ind Eng Chem Res*. 2010;49(7):3286–3294.
51. Cardoso SR, Barbosa-Póvoa AP, Relvas S. Integrating financial risk measures into the design and planning of closed-loop supply chains. *Comp Chem Eng*. 2016;85:105–123.
52. You F, Wassick JM, Grossmann IE. Risk management for a global supply chain planning under uncertainty: models and algorithms. *AIChE J*. 2009;55(4):931–946.
53. Chaoyue Z, Yongpei G. Unified stochastic and robust unit commitment. *Power Syst IEEE Trans*. 2013;28(3):3353–3361.
54. McLean K, Li X. Robust scenario formulations for strategic supply chain optimization under uncertainty. *Ind Eng Chem Res*. 2013; 52(16):5721–5734.
55. Cong L, Changhyeok L, Haoyong C, Mehrotra S. Stochastic robust mathematical programming model for power system optimization. *Power Syst IEEE Trans*. 2016;31(1):821–822.
56. Ben-Tal A, Goryashko A, Guslitzer E, Nemirovski A. Adjustable robust solutions of uncertain linear programs. *Math Prog*. 2003; 99(2):351–376.
57. UNCTAD. *The State of the Biofuels Market: Regulatory, Trade and Development Perspectives*. United Nations: UNCTAD.
58. You F, Tao L, Graziano DJ, Snyder SW. Optimal design of sustainable cellulosic biofuel supply chains: multiobjective optimization coupled with life cycle assessment and input–output analysis. *AIChE J*. 2012;58(4):1157–1180.
59. An H, Wilhelm WE, Searcy SW. Biofuel and petroleum-based fuel supply chain research: a literature review. *Biomass Bioenerg*. 2011; 35(9):3763–3774.
60. Awudu I, Zhang J. Uncertainties and sustainability concepts in biofuel supply chain management: a review. *Renew Sustain Energ Rev*. 2012;16(2):1359–1368.
61. Yue D, Kim MA, You F. Design of sustainable product systems and supply chains with life cycle optimization based on functional unit: general modeling framework, mixed-integer nonlinear programming algorithms and case study on hydrocarbon biofuels. *ACS Sustain Chem Eng*. 2013;1(8):1003–1014.
62. Akgul O, Shah N, Papageorgiou LG. Economic optimisation of a UK advanced biofuel supply chain. *Biomass Bioenerg*. 2012;41:57–72.
63. Alex Marvin W, Schmidt LD, Benjaafar S, Tiffany DG, Daoutidis P. Economic optimization of a lignocellulosic biomass-to-ethanol supply chain. *Chem Eng Sci*. 2012;67(1):68–79.
64. Andersen FE, Díaz MS, Grossmann IE. Multiscale strategic planning model for the design of integrated ethanol and gasoline supply chain. *AIChE J*. 2013;59(12):4655–4672.
65. Dunnett AJ, Adjiman CS, Shah N. A spatially explicit whole-system model of the lignocellulosic bioethanol supply chain: an assessment of decentralised processing potential. *Biotechnol Biofuel*. 2008;1(1):1–17.
66. Giarola S, Zamboni A, Bezzo F. Spatially explicit multi-objective optimisation for design and planning of hybrid first and second generation biorefineries. *Comp Chem Eng*. 2011;35(9):1782–1797.
67. El-Halwagi AM, Rosas C, Ponce-Ortega JM, Jiménez-Gutiérrez A, Mannan MS, El-Halwagi MM. Multiobjective optimization of biorefineries with economic and safety objectives. *AIChE J*. 2013;59(7): 2427–2434.
68. Liu P, Georgiadis MC, Pistikopoulos EN. Advances in energy systems engineering. *Ind Eng Chem Res*. 2011;50(9):4915–4926.
69. Santibañez-Aguilar JE, González-Campos JB, Ponce-Ortega JM, Serna-González M, El-Halwagi MM. Optimal planning of a biomass conversion system considering economic and environmental aspects. *Ind Eng Chem Res*. 2011;50(14):8558–8570.
70. You F, Wang B. Life cycle optimization of biomass-to-liquid supply chains with distributed–centralized processing networks. *Ind Eng Chem Res*. 2011;50(17):10102–10127.
71. Yue D, Pandya S, You F. Integrating hybrid life cycle assessment with multiobjective optimization: a modeling framework. *Environ Sci Technol*. 2016;50(3):1501–1509.
72. Yue D, Slivinsky M, Sumpter J, You F. Sustainable design and operation of cellulosic bioelectricity supply chain networks with life cycle economic, environmental, and social optimization. *Ind Eng Chem Res*. 2014;53(10):4008–4029.
73. Bai Y, Ouyang Y, Pang J-S. Biofuel supply chain design under competitive agricultural land use and feedstock market equilibrium. *Energ Econ*. 2012;34(5):1623–1633.
74. Yeh K, Realff MJ, Lee JH, Whittaker C. Analysis and comparison of single period single level and bilevel programming representations of a pre-existing timberlands supply chain with a new biorefinery facility. *Comp Chem Eng*. 2014;68:242–254.
75. Yue D, You F. Game-theoretic modeling and optimization of multi-echelon supply chain design and operation under Stackelberg game and market equilibrium. *Comp Chem Eng*. 2014;71:347–361.
76. Yue D, You F. Fair profit allocation in supply chain optimization with transfer price and revenue sharing: MINLP model and algorithm for cellulosic biofuel supply chains. *AIChE J*. 2014;60(9): 3211–3229.
77. Dal-Mas M, Giarola S, Zamboni A, Bezzo F. Strategic design and investment capacity planning of the ethanol supply chain under price uncertainty. *Biomass Bioenerg*. 2011;35(5):2059–2071.
78. Osmani A, Zhang J. Stochastic optimization of a multi-feedstock lignocellulosic-based bioethanol supply chain under multiple uncertainties. *Energy*. 2013;59:157–172.
79. Hamelinck CN, Hooijdonk GV, Faaij APC. Ethanol from lignocellulosic biomass: techno-economic performance in short-, middle- and long-term. *Biomass Bioenerg*. 2005;28(4):384–410.
80. USDA. Field Crops Usual Planting and Harvesting Dates. *United States Department of Agriculture, National Agricultural Statistics Service*. 2010; Agricultural Handbook Number 628.
81. NASS. National Agricultural Statistics Service. 2012.
82. EIA. U.S. Energy Information Adminstration. www. eia.doe/gov.
83. U.S. Census Bureau. http://www.census.gov. Accessed October 18, 2012.
84. Searcy E, Flynn P, Ghafoori E, Kumar A. The relative cost of biomass energy transport. *Appl Biochem Biotech*. 2007;137:639–652.
85. Mahmudi H, Flynn PC. Rail vs truck transport of biomass. *Appl Biochem Biotechnol*. 2006;129–132.
86. Ben-Tal A, El Ghaoui L, Nemirovski A. *Robust Optimization*. Princeton: Princeton University Press; 2009.
87. Rosenthal RE. *GAMS—A User's Guide*. Washington, DC: GAMS Development Corp., 2011.
88. Atamtürk A, Zhang M. Two-stage robust network flow and design under demand uncertainty. *Operat Res*. 2007;55(4):662–673.

Appendix A: Improved C&CG Algorithm

The improved C&CG algorithm involves multiple max–min problems (i.e., one for each scenario) at the second stage. Because the scenarios in problem (P1) are independent to each other and the variables u_s and z_s are all scenario-dependent, the C&CG algorithm is still valid for solving problem (P1). For ease of exposition, we impose the relatively complete recourse assumption that the second-stage optimization problem is feasible for any given y and u_s. Whereas, problems that do not satisfy the relatively complete recourse assumption can still be coped with using the C&CG algorithm by considering feasibility cuts in addition to optimality cuts.[8]

To facilitate the application of C&CG algorithm, we defined the uncertainty set for operational uncertainties in each scenario as follows, which is a popular way to handle the uncertainty in supply availability, demand level, etc.[29,88]

$$U_s=\left\{\begin{array}{l} u_s : u_s^{(j)}=\underline{u}_s^{(j)}+G_s^{(j)}\tilde{u}_s^{(j)} \\ \qquad \sum_j G_s^{(j)} \le \Gamma \\ \qquad G_s^{(j)} \in [0,1], j=1,\ldots,n \end{array}\right\}, \forall s \in S \qquad (\mathbf{US})$$

where the superscript (j) indicates the jth element of a vector; $\underline{u}_s^{(j)}$ is the basic level of uncertainty; $\tilde{u}_s^{(j)}$ is the maximal deviation; and Γ is a predefined integer value in the constraint of budget uncertainty to control the level of conservativeness. $G_s^{(j)}$ is a continuous variable between 0 and 1, of which the value reflects the level of operational uncertainty $u_s^{(j)}$ between the basic and maximum levels.

It can be proved that if the uncertainty set U_s is a polyhedron, as in the case of (US), the value of u_s at the optimal solution will be at one of the extreme points of the polyhedron.[8] Therefore, if we enumerate all the extreme points and index them with $l \in L$, then

the original two-stage problem (P1) can be reduced to an equivalent (probably large-scale) mixed integer program as follows.

$$\begin{aligned}
\min \quad & C^{str}(x,y)+\sum_{s\in S} p_s \overline{C}_s^{opr}(x,y) \\
\text{s.t.} \quad & Ax+By \geq d \\
& x\in\{0,1\}^n, y\in\mathbb{R}^m \\
& \left\{\begin{array}{l} \overline{C}_s^{opr}(x,y) \geq C_{s,l}^{opr}\left(x,y,z_{s,l}\right) \\ Gz_{s,l} \geq h_s - E_s x - F_s y - K_s u_{s,l} \\ z_s \in \mathbb{R}^r \end{array}\right\}, \forall s\in S, l\in L
\end{aligned} \tag{P2}$$

where $u_{s,l}$ represents a particular extreme point of uncertainty set (US), which is also a particular realization of the operational uncertainty; $z_{,l}$ is the corresponding recourse variable under the realization of strategic uncertainty in scenario s and operational uncertainty at extreme point l. A critical issue about equivalent formulation (P2) is that when the number of extreme points is very large it might not be practically feasible to derive the optimal solution, because the size of problem (P2) can be computationally intractable. Consequently, the C&CG algorithm was developed based on the idea of partial enumeration and implemented in a master-subproblem framework. The master problem is given by,

$$\begin{aligned}
\min \quad & C^{str}(x,y)+\sum_{s\in S} p_s \overline{C}_s^{opr}(x,y) \\
\text{s.t.} \quad & Ax+By \geq d \\
& x\in\{0,1\}^n, y\in\mathbb{R}^m \\
& \left\{\begin{array}{l} \overline{C}_s^{opr}(x,y) \geq C_{s,l}^{opr}\left(x,y,z_{s,l}\right) \\ Gz_{s,l} \geq h_s - E_s x - F_s y - K_s u_{s,l} \\ z_s \in \mathbb{R}^r \end{array}\right\}, \forall s\in S, l\in \underline{L}\subset L
\end{aligned} \tag{MP}$$

where $\underline{L}$ is a subset of set L. As can be seen, the master problem (MP) is almost the same as the equivalent mixed integer program (P2). The difference lies in that only a partial enumeration of the extreme points of uncertainty set (US) is considered, i.e., $l\in\underline{L}\subset L$. It is straightforward to see that problem (MP) is a valid relaxation of problem (P1), thus providing a lower bound to the original two-stage problem (P1). Therefore, expanding the partial enumeration $\underline{L}$ by adding significant extreme points $u_{s,l}$ iteratively would lead to a sequence of increasing lower bounds. It is worth noting that the master problem (MP) possesses a decomposable structure, which can be exploited by Benders decomposition when the number of scenarios are very large.[13,14,21]

For the proposed stochastic robust optimization model, there is a subproblem for each scenario s of the strategic uncertainty realization. A general form is given by,

$$\begin{aligned}
& \left\{\begin{array}{ll} \overline{C}_s^{opr}(x,y)= \max\limits_{u_s\in U_s} \min\limits_{z} & C_s^{opr}(x,y,z_s,u_s) \\ \text{s.t.} & Gz_s \geq h_s - E_s x - F_s y - K_s u_s \\ & z_s\in\mathbb{R}^r \end{array}\right\}, \\
& \forall s\in S
\end{aligned} \tag{SP}$$

The optimal solution of subproblem (SP) provides the worst-case operational cost given the first-stage plan (x,y) and the realization of strategic uncertainty in scenario s. Therefore, combining $\overline{C}_s^{opr}(x,y)$ over different scenarios plus the first-stage cost would provide an upper bound to the original two-stage problem (P1). The max–min subproblem (SP) can be solved based on either KKT-conditions or strong duality.[8] The idea of both approaches is to transform the max–min problem into a mixed integer program. Proof of convergence of the C&CG algorithm can be found in the article by Zeng and Zhao.[8] An intuitive interpretation of the proof is that because the number of extreme points of uncertainty set (US) is finite and a different extreme point is guaranteed to emerge in each iteration if termination criterion is not met, the C&CG algorithm terminates in a finite number of iterations.

Appendix B: Model Formulations of the Case Study

Master problem

The master problem to be employed in the C&CG algorithm is given below, which is formulated as an MILP. The objective function is (B1) and the constraints include (B2)–(B17). The objective (B1) is to minimize the annualized total cost, which covers the first-stage cost and an expectation of the second-stage cost.

$$\min \quad TC = C^{fix} + \sum_{s\in S} prb_s \cdot C_s^{opr} \tag{B1}$$

The first-stage constraints include (B2)–(B6). Constraint (B2) enforces that only one capacity level and one conversion technology can be chosen at a particular biorefinery. Constraint (B3) specifies the lower and upper bounds of each capacity level. Constraints (B4) and (B5) calculates the capital investment and fixed O&M cost, respectively, according to the piecewise linear cost function. Equation (B6) calculates the annualized first-stage cost.

$$\sum_{r\in R}\sum_{g\in G} X_{j,r,g} \leq 1, \quad \forall j\in J \tag{B2}$$

$$pr_{j,r-1,g}\cdot X_{j,r,g} \leq Cp_{j,r,g} \leq pr_{j,r,g}\cdot X_{j,r,g}, \quad \forall j\in J, r\in R, g\in G \tag{B3}$$

$$Inv_j = \sum_{r\in R}\sum_{g\in G}\left[cr_{j,r-1,g}\cdot X_{j,r,g} + \frac{\left(Cp_{j,r,g}-pr_{j,r-1,g}\cdot X_{j,r,g}\right)\left(cr_{j,r,g}-cr_{j,r-1,g}\right)}{pr_{j,r,g}-pr_{j,r-1,g}}\right], \quad \forall j\in J \tag{B4}$$

$$Omc_j = \sum_{g\in G} cf_g \cdot \sum_{r\in R}\left[cr_{j,r-1,g}\cdot X_{j,r,g} + \frac{\left(Cp_{j,r,g}-pr_{j,r-1,g}\cdot X_{j,r,g}\right)\left(cr_{j,r,g}-cr_{j,r-1,g}\right)}{pr_{j,r,g}-pr_{j,r-1,g}}\right], \quad \forall j\in J \tag{B5}$$

$$C^{fix} = ann \sum_{j \in J} Inv_j + \sum_{j \in J} Omc_j \tag{B6}$$

The second stage constraints include (B7)–(B15). Constraint (B7) indicates that the worst-case second-stage cost should be no less than the total operational cost under any realization l (extreme point of the uncertainty set) of the operational uncertainties. The total operational cost covers biomass acquisition, biofuel production, transportation and inventory holding of both biomass and biofuel, as well as the penalty cost for using fuel ethanol from the external source to satisfy the demand.

$$\begin{aligned} C_s^{opr} \geq & \sum_{b \in B} \sum_{i \in I} \sum_{t \in T} pcc_{b,i,t} \cdot Pb_{b,i,t,s,l} \\ & + \sum_{p \in P} \sum_{j \in J} \sum_{t \in T} \sum_{g \in G} cm_{p,j,t,g} \cdot Wp_{p,j,t,s,g,l} \\ & + \sum_{b \in B} \sum_{i \in I} \sum_{j \in J} \sum_{t \in T} \frac{ctb_{b,i,j} \cdot Fb_{b,i,j,t,s,l}}{1 - mcb_b} + \sum_{p \in P} \sum_{j \in J} \sum_{k \in K} \sum_{t \in T} ctp_{p,j,k} \cdot Fp_{p,j,k,t,s,l} \\ & + \sum_{b \in B} \sum_{j \in J} \sum_{t \in T} h_t \cdot hb_{b,j,t} \cdot Sb_{b,j,t,s,l} + \sum_{p \in P} \sum_{j \in J} \sum_{t \in T} h_t \cdot hp_{p,j,t} \cdot Sp_{p,j,t,s,l} \\ & + \sum_{p \in P} \sum_{k \in K} \sum_{t \in T} cim_{p,k,t} \cdot Ep_{p,k,t,s,l} \end{aligned} \tag{B7}$$

Constraint (B8) indicates that the purchasing amount of biomass cannot exceed the availability at the suppliers. Constraint (B9) indicates that all purchased biomass is shipped to biorefineries in the same time period. Note that combining (B8) and (B9) can eliminate the variable $Pb_{b,i,t,s,l}$. The parameter of biomass availability $\hat{a}_{b,i,t,s,l}$ represents a particular realization l of operational uncertainty in scenario s.

$$Pb_{b,i,t,s,l} \leq \hat{a}_{b,i,t,s,l}, \qquad \forall b \in B, i \in I, t \in T, s \in S, l \in L \tag{B8}$$

$$Pb_{b,i,t,s,l} = \sum_{j \in J} Fb_{b,i,j,t,s,l}, \qquad \forall b \in B, i \in I, t \in T, s \in S, l \in L \tag{B9}$$

Constraint (B10) models the mass balance of biomass at biorefineries, where degradation of biomass is explicitly accounted for by the degradation factor $\psi_{b,j,t}$.

$$\left(1 - \psi_{b,j,t}\right) Sb_{b,j,t--1,s,l} + \sum_{i \in I} Fb_{b,i,j,t,s,l} = Sb_{b,j,t,s,l} + \sum_{g \in G} Wb_{b,j,t,s,g,l}, \quad \forall b \in B, j \in J, t \in T, s \in S, l \in L \tag{B10}$$

Constraint (B11) states that the biofuel production level can neither exceed the capacity nor fall below the minimum utilization rate, if $\eta_j > 0$.

$$\eta_j \frac{h_t}{rt} \sum_{r \in R} Cp_{j,r,g} \leq \sum_{p \in P} \varphi_p \cdot Wp_{p,j,t,s,g,l} \leq \frac{h_t}{rt} \sum_{r \in R} Cp_{j,r,g}, \quad \forall j \in J, t \in T, s \in S, g \in G, l \in L \tag{B11}$$

Conversion from biomass to biofuel is modeled by (B12). Note that the conversion efficiency $\hat{\alpha}_{b,p,s,g}$ is one of the strategic uncertainty considered. Therefore, its value is scenario dependent.

$$Wp_{p,j,t,s,g,l} = \sum_{b \in B} \hat{\alpha}_{b,p,s,g} \cdot Wb_{b,j,t,s,g,l}, \quad \forall p \in P, j \in J, t \in T, s \in S, g \in G, l \in L \tag{B12}$$

Constraint (B13) models the mass balance of biofuel at biorefineries.

$$Sp_{p,j,t--1,s,l} + \sum_{g \in G} Wp_{p,j,t,s,g,l} = Sp_{p,j,t,s,l} + \sum_{k \in K} Fp_{p,j,k,t,s,l}, \quad \forall p \in P, j \in J, t \in T, s \in S, l \in L \tag{B13}$$

Constraint (B14) indicates that the biofuel shipped to a biofuel customer must be all sold. Constraint (B15) indicates that the demand must be satisfied either from the internal production or from an external source with high penalty. Note that combining (B14) and (B15) can eliminate variable $Sd_{p,k,t,s,l}$. The parameter of demand $\hat{d}_{p,k,t,s,l}$ represents a particular realization l of operational uncertainty in scenario s.

$$Sd_{p,k,t,s,l} = \sum_{j \in J} Fp_{p,j,k,t,s,l}, \qquad \forall p \in P, k \in K, t \in T, s \in S, l \in L \tag{B14}$$

$$Sd_{p,k,t,s,l} + Ep_{p,k,t,s,l} \geq \hat{d}_{p,k,t,s,l}, \quad \forall p \in P, k \in K, t \in T, s \in S, l \in L \tag{B15}$$

The first-stage variables are given in (B16) and the second-stage variables are given in (B17).

$$X_{j,r,g} \in \{0,1\}, Cp_{j,r,g} \in \mathbb{R}^+ \tag{B16}$$

$$Pb_{b,i,t,s,l}, Fb_{b,i,j,t,s,l}, Sb_{b,j,t,s,l}, Wb_{b,j,t,s,g,l}, Wp_{p,j,t,s,g,l}, Sp_{p,j,t,s,l}, Sd_{p,k,t,s,l}, Ep_{p,k,t,s,l} \in \mathbb{R}^+ \tag{B17}$$

Subproblem

The subproblem to be employed in the C&CG algorithm is presented in this section, which is an MILP developed based on strong duality. The objective is (B18) and the constraints include (B19)–(B35). Note that we will be solving this subproblem for each scenario of the strategic uncertainty.

$$\max \quad C^{robust} = -\sum_{b\in B}\sum_{i\in I}\sum_{t\in T}\underline{a}_{b,i,t}\cdot D^{av}_{b,i,t} + \tilde{a}_{b,i,t}\cdot Gad^{av}_{b,i,t} + \sum_{j\in J}\sum_{t\in T}\sum_{g\in G}\frac{h_t}{rt}capx_{j,g}\left(\eta_j\cdot D^{cpl}_{j,t,g} - D^{cpu}_{j,t,g}\right) + \sum_{p\in P}\sum_{k\in K}\sum_{t\in T}\underline{d}_{p,k,t}\cdot D^{im}_{p,k,t} + \tilde{d}_{p,k,t}\cdot Gdd^{im}_{p,k,t} \tag{B18}$$

Constraints (B19)–(B21) are for the Glover's linearization of $Gad^{av}_{b,i,t} = Ga_{b,i}\cdot D^{av}_{b,i,t}$. Constraints (B22)–(B24) are for the Glover's linearization of $Gdd^{im}_{p,k,t} = Gd_{p,k}\cdot D^{im}_{p,k,t}$.

$$Gad^{av}_{b,i,t} \le D^{av}_{b,i,t}, \qquad \forall b\in B, i\in I, t\in T \tag{B19}$$

$$Gad^{av}_{b,i,t} \le M\cdot Ga_{b,i}, \qquad \forall b\in B, i\in I, t\in T \tag{B20}$$

$$Gad^{av}_{b,i,t} \ge D^{av}_{b,i,t} - M\left(1-Ga_{b,i}\right), \qquad \forall b\in B, i\in I, t\in T \tag{B21}$$

$$Gdd^{im}_{p,k,t} \le D^{im}_{p,k,t}, \qquad \forall p\in P, k\in K, t\in T \tag{B22}$$

$$Gdd^{im}_{p,k,t} \le M\cdot Gd_{p,k}, \qquad \forall p\in P, k\in K, t\in T \tag{B23}$$

$$Gdd^{im}_{p,k,t} \ge D^{im}_{p,k,t} - M\left(1-Gd_{p,k}\right), \qquad \forall p\in P, k\in K, t\in T \tag{B24}$$

The constraint of budget uncertainty for biomass availability is given by (B25), and that for biofuel demand is given by (B26).

$$\sum_{i\in I}\left(1-Ga_{b,i}\right) \le \Gamma a_b, \qquad \forall b\in B \tag{B25}$$

$$\sum_{k\in K}Gd_{p,k} \le \Gamma d_p, \qquad \forall p\in P \tag{B26}$$

The dual constraints include (B27)–(B33). From top to bottom, the dual constraints correspond to the primal variables *Fb*, *Sb*, *Wb*, *Wp*, *Sp*, *Fp*, and *Ep*, respectively. As aforementioned, the primal variables *Pb* and *Sd* are eliminated by combining the constraints.

$$-D^{av}_{b,i,t} + D^{bm}_{b,j,t} \le pcc_{b,i,t} + \frac{ctb_{b,i,j}}{1-mcb_b}, \qquad \forall b\in B, i\in I, j\in J, t\in T \tag{B27}$$

$$\left(1-\psi_{b,j,t++1}\right)\cdot D^{bm}_{b,j,t++1,s} - D^{bm}_{b,j,t,s} \le h_t\cdot hb_{b,j,t}, \qquad \forall b\in B, j\in J, t\in T \tag{B28}$$

$$-D^{bm}_{b,j,t} - \sum_{p\in P}\beta_{b,p,g}\cdot D^{con}_{p,j,t,g} \le 0, \qquad \forall b\in B, j\in J, t\in T, g\in G \tag{B29}$$

$$\varphi_p\left(D^{cpl}_{j,t,g} - D^{cpu}_{j,t,g}\right) + D^{con}_{p,j,t,g} + D^{pm}_{p,j,t} \le cm_{p,j,t,g}, \qquad \forall p\in P, j\in J, t\in T, g\in G \tag{B30}$$

$$D^{pm}_{p,j,t++1} - D^{pm}_{p,j,t} \le h_t\cdot hp_{p,j,t}, \qquad \forall p\in P, j\in J, t\in T \tag{B31}$$

$$-D^{pm}_{p,j,t} + D^{im}_{p,k,t} \le ctp_{p,j,k}, \qquad \forall p\in P, j\in J, k\in K, t\in T \tag{B32}$$

$$D^{im}_{p,k,t} \le cim_{p,k,t}, \qquad \forall p\in P, k\in K, t\in T \tag{B33}$$

The nonnegative and free dual variables are listed in (B34) and the uncertainty-set related variables are given in (B35). When the budgets of uncertainty, Γa_b and Γd_p, are set to integer values, $Ga_{b,i}$ and $Gd_{p,k}$ can be considered binary variables, because they will always be equal to either 0 or 1 at any optimal solutions.

$$D^{av}_{b,i,t}, D^{cpl}_{j,t,g}, D^{cpu}_{j,t,g}, D^{im}_{p,k,t} \in \mathbb{R}^+; D^{bm}_{b,j,t}, D^{con}_{p,j,t,g}, D^{pm}_{p,j,t} \in \mathbb{R} \tag{B34}$$

$$Gad^{av}_{b,i,t}, Gdd^{im}_{p,k,t} \in \mathbb{R}^+; Ga_{b,i}, Gd_{p,k} \in \{0,1\} \tag{B35}$$

Manuscript received Feb. 19, 2016, and revision received Mar. 23, 2016.